FAA-79-21.II
REPORT NO. FAA-EM-79-11, II

THEORETICAL STUDIES OF MICROSTRIP ANTENNAS
Volume II: Analysis and Synthesis of Multi-Frequency Elements

Frederic R. Morgenthaler
71 Abbott Road
Wellesley MA 02181

SEPTEMBER 1979

FINAL REPORT

Prepared for
U.S. DEPARTMENT OF TRANSPORTATION
FEDERAL AVIATION ADMINISTRATION
Office of Systems Engineering Management
Washington DC 20591

NOTICE

This document is disseminated under the sponsorship of the Department of Transportation in the interest of information exchange. The United States Government assumes no liability for its contents or use thereof.

NOTICE

The United States Government does not endorse products or manufacturers. Trade or manufacturers' names appear herein solely because they are considered essential to the object of this report.

Technical Report Documentation Page

1. Report No.	2. Government Accession No.	3. Recipient's Catalog No.
FAA-EM-79-11, II		

4. Title and Subtitle	5. Report Date
THEORETICAL STUDIES OF MICROSTRIP ANTENNAS Volume II: Analysis and Synthesis of Multi-Frequency Elements	September 1979
	6. Performing Organization Code
7. Author(s) Frederic R. Morgenthaler	8. Performing Organization Report No. DOT-TSC-FAA-79-21, II
9. Performing Organization Name and Address Frederic R. Morgenthaler* 71 Abbott Road Wellesley MA 02181	10. Work Unit No. (TRAIS) FA 957/R9138
	11. Contract or Grant No. DOT-TS-15364-2
	13. Type of Report and Period Covered Final Report April 1978 - July 1979
12. Sponsoring Agency Name and Address U.S. Department of Transportation Federal Aviation Administration Office of Systems Engineering Management Washington DC 20591	14. Sponsoring Agency Code

15. Supplementary Notes
*Under Contract to: U.S. Department of Transportation
Research and Special Programs Administration
Transportation Systems Center
Cambridge MA 02142

16. Abstract Volume II of Theoretical Studies of Microstrip Antennas deals with the analysis and synthesis of several types of novel multi-resonant elements with emphasis on dual-frequency operation of rectangular microstrip patch antennas with or without external matching networks.

Specifically, we analyze dual resonances created within a single rectangular patch by means of appropriate dielectric loading and also those associated with a patch capacitively-coupled to either a lumped or distributed matching network. In all cases radiation is obtained from slots in the rectangular patch in combination with open-circuited edges.

Rather than separately design the dual-resonating elements and matching networks and hope for efficient radiation and proper patterns at both frequencies, we favor and herein pursue an integrated synthesis which demands simultaneous fulfillment of the design goals.

A synthesis approach, based upon coupled resonator theory, is also developed and applied to situations in which one resonant element is a rectangular microstrip patch and the second element either a second patch or else a lumped or distributed matching network. Based upon these considerations, several new antenna configurations are proposed that utilize either in line or stacked element geometries.

Volume I of this report deals with general design techniques and analyses of single and coupled microstrip radiating elements.

17. Key Words	18. Distribution Statement
Microstrip Antennas Microstrip Analysis Multi-frequency Antennas	DOCUMENT IS AVAILABLE TO THE PUBLIC THROUGH THE NATIONAL TECHNICAL INFORMATION SERVICE, SPRINGFIELD, VIRGINIA 22161

19. Security Classif. (of this report)	20. Security Classif. (of this page)	21. No. of Pages	22. Price
Unclassified	Unclassified	50	

Form DOT F 1700.7 (8-72) Reproduction of completed page authorized

PREFACE

Compact microwave antennas formed from resonant microstrip elements have recently attracted considerable attention because of their simplicity and conformability to shaped surfaces.

The Department of Transportation has been especially interested in this type of antenna for possible application with the Global Positioning System (GPS) and in aircraft satellite communications systems.

The work reported in both Volumes I and II of this document is aimed at providing a general theoretical framework useful for analyzing and/or synthesizing microstrip antennas and arrays. The work was completed and this report prepared by F. R. Morgenthaler under the direction of TSC Technical Monitor Leslie Klein.

METRIC CONVERSION FACTORS

Approximate Conversions to Metric Measures

Symbol	When You Know	Multiply by	To Find	Symbol
		LENGTH		
in	inches	2.5	centimeters	cm
ft	feet	30	centimeters	cm
yd	yards	0.9	meters	m
mi	miles	1.6	kilometers	km
		AREA		
in^2	square inches	6.5	square centimeters	cm^2
ft^2	square feet	0.09	square meters	m^2
yd^2	square yards	0.8	square meters	m^2
mi^2	square miles	2.6	square kilometers	km^2
	acres	0.4	hectares	ha
		MASS (weight)		
oz	ounces	28	grams	g
lb	pounds	0.45	kilograms	kg
	short tons (2000 lb)	0.9	tonnes	t
		VOLUME		
tsp	teaspoons	5	milliliters	ml
Tbsp	tablespoons	15	milliliters	ml
fl oz	fluid ounces	30	milliliters	ml
c	cups	0.24	liters	l
pt	pints	0.47	liters	l
qt	quarts	0.95	liters	l
gal	gallons	3.8	liters	l
ft^3	cubic feet	0.03	cubic meters	m^3
yd^3	cubic yards	0.76	cubic meters	m^3
		TEMPERATURE (exact)		
°F	Fahrenheit temperature	5/9 (after subtracting 32)	Celsius temperature	°C

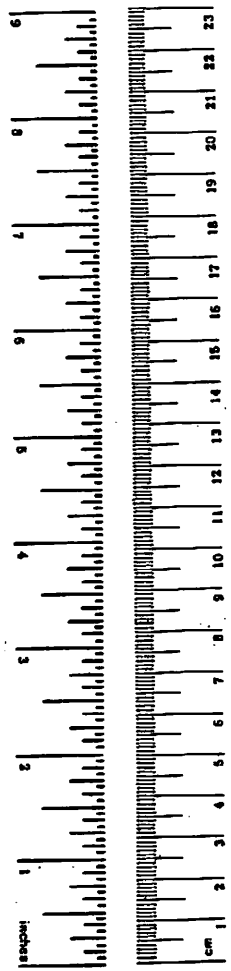

Approximate Conversions from Metric Measures

Symbol	When You Know	Multiply by	To Find	Symbol
		LENGTH		
mm	millimeters	0.04	inches	in
cm	centimeters	0.4	inches	in
m	meters	3.3	feet	ft
m	meters	1.1	yards	yd
km	kilometers	0.6	miles	mi
		AREA		
cm^2	square centimeters	0.16	square inches	in^2
m^2	square meters	1.2	square yards	yd^2
km^2	square kilometers	0.4	square miles	mi^2
ha	hectares (10,000 m^2)	2.5	acres	
		MASS (weight)		
g	grams	0.035	ounces	oz
kg	kilograms	2.2	pounds	lb
t	tonnes (1000 kg)	1.1	short tons	
		VOLUME		
ml	milliliters	0.03	fluid ounces	fl oz
l	liters	2.1	pints	pt
l	liters	1.06	quarts	qt
l	liters	0.26	gallons	gal
m^3	cubic meters	35	cubic feet	ft^3
m^3	cubic meters	1.3	cubic yards	yd^3
		TEMPERATURE (exact)		
°C	Celsius temperature	9/5 (then add 32)	Fahrenheit temperature	°F

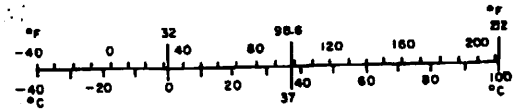

TABLE OF CONTENTS

LIST OF ILLUSTRATIONS

EXECUTIVE SUMMARY

Microwave antennas formed from resonant microstrip elements have recently attracted considerable attention because of their conformability to shaped surfaces and their compactness and simplicity.

In order to accomodate dual-frequency operation, Ball Aerospace Systems has developed the stacked element concept in which the smaller high frequency patch is placed above the larger, low-frequency patch. A discussion of the unwanted coupling between such patches was included in Volume I of this report. It is most severe when the two frequencies are closely spaced.

Rather than separately design the dual-resonating elements and matching networks and hope for efficient radiation and proper patterns at both frequencies, we favor and herein pursue an integrated synthesis which demands simultaneous fulfillment of the design goals.

In this second volume, we discuss and analyze an alternate approach in which the dual resonances are created within a single rectangular patch by means of appropriate dielectric loading and the use of radiating slots.

In particular, we develop a theoretical modal to describe the approximate electromagnetic mode structure of a rectangular patch loaded symmetrically with up to three dielectric slabs that serve to concentrate the rf energy.

Both even and odd modes are considered and the modal field distributions are used to derive the radiation pattern produced by a radiating edge or a slot in the top plate of a multi-resonant rectangular patch.

Dual resonances in rectangular microstrip patch filled with homogeneous dielectric are shown to be practical when the desired separation between frequencies is at least 5-10 percent.

A synthesis approach, based upon coupled resonator theory, is also de-

veloped and applied to situations in which one resonant element is a rectangular microstrip patch and the second element either a second patch or else a lumped or distributed matching network. Based upon these considerations, several new antenna configurations are proposed that utilize either in line or stacked element geometries. It is also noted that if lumped capacitive coupling is provided by reversed bias varactor-type diodes, the frequency separation between modes can be made electronically tunable through bias voltage control.

1. INTRODUCTION

The microstrip antenna under consideration has the basic geometry shown in Fig. 1 and consists of one or more perfectly conducting metal patches deposited upon the surface of a dielectric slab backed by a perfectly conducting ground plane. The sandwich is surrounded by free space.

The basic characteristics of a rectangular microstrip patch such as that shown in Fig. 2 have been reviewed in the first volume* of this report.

When radiation at two or more closely spaced frequencies is required, there are several strategies that can be followed.

If the frequency spacing is very small, it is probably best simply to broaden the main resonance of a single patch by lowering the overall Q, with some combination of increased slab thickness and lowered dielectric constant.

If the desired frequency separation is moderate - greater than a few percent - external frequency sensitive matching networks can be employed perhaps possibly in connection with separate radiating elements designed for each frequency.

In order to accommodate dual-frequency operation, Ball Aerospace Systems** has developed the stacked element concept in which the smaller high frequency patch is placed above the larger, low-frequency patch. A discussion of the coupling between such patches was also included in Volume I of this report.

An alternate approach, and the one first discussed and analyzed here, relies upon suitable design of the basic micro-patch element so that it will

---

* Morgenthaler, F.R., "Theoretical Studies of Microstrip Antennas, Volume I, General Design Techniques and Analyses of Single and Coupled Elements."

** Sanford, G., "Advanced Microstrip Phased Array Technology Development," DOT-TSC, Report in Preparation.

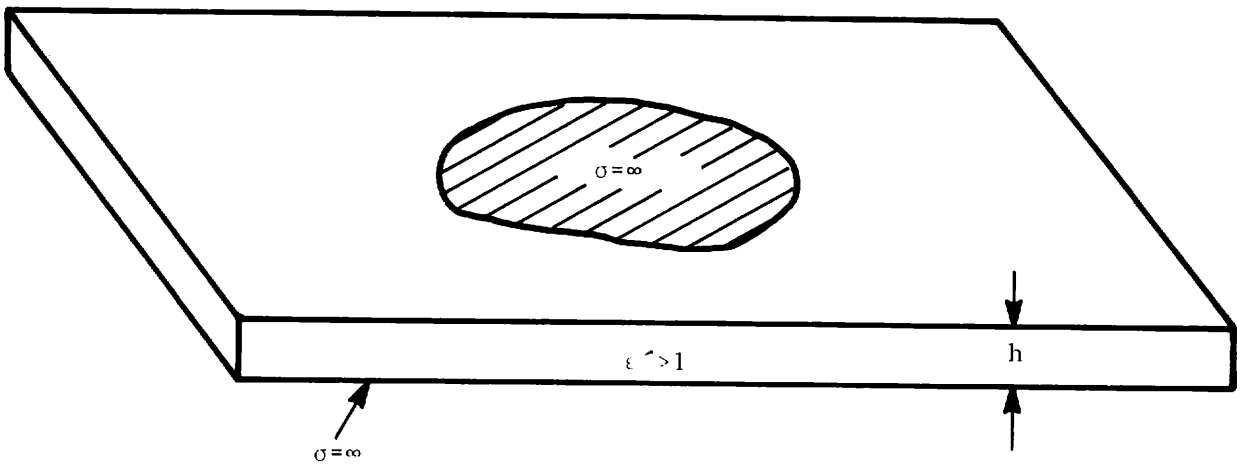

The conducting plane ($y = -h$) and strip ($y = 0$, $|x| \leq w/2$) are assumed to have infinite conductivity and zero thickness; the slab of dielectric constant $\varepsilon' \geq 1$ and thickness h is assumed lossless.

FIGURE 1. MICROSTRIP GEOMETRY SHOWN IN CROSS SECTION

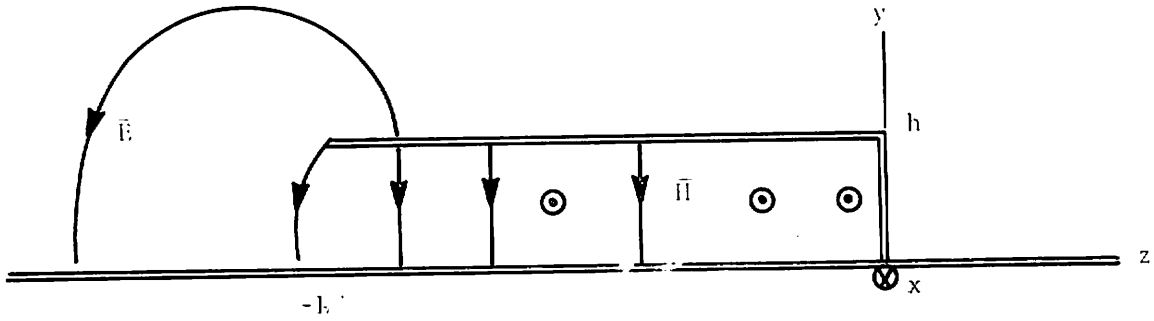

(a)

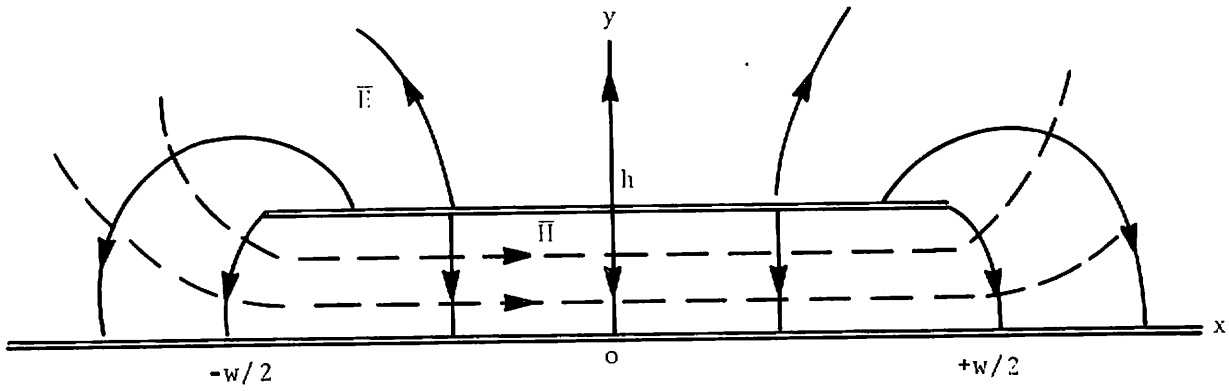

(b)

Two microstrip patches of width w_1 and w_2, both spaced a distance h above the same ground plane, parallel to one another and separated by a distance ℓ.

FIGURE 2. TWO COUPLED MICROSTRIP PATCHES

be resonant at both desired frequencies, and moreover, that these eigenmodes will each radiate efficiently with appropriate patterns.

As it were, the micropatch provides its own matching network by means of the internal mode structure.

In particular, we develop a theoretical model to describe the approximate electromagnetic mode structure of a rectangular patch loaded symmetrically with up to three dielectric slabs that serve to concentrate the rf energy.

Both even and odd modes are considered and the modal field distribution used to derive the radiation pattern produced by a radiation edge or a slot in the top plate of a multi-resonant rectangular patch.

Dual resonances in rectangular microstrip patch filled with homogeneous dielectric are shown to be practical when the desired separation between frequencies is at least 5 - 10 percent.

It can be expected that the additional flexibility will require somewhat larger patch area but the use of high dielectric constant slab loading can help reduce such increases in "real estate". Such loading will tend to increase each individual resonance Q; if required this can be compensated for by increasing the dielectric thickness.

A second synthesis approach to the problem is also considered. It is based upon coupled resonator theory and is also developed and applied to situations in which one resonant element is a rectangular microstrip patch and the second element either a second patch or else a lumped or distributed matching network. Based upon these considerations, several new antenna configurations are proposed that utilize either in line or stacked element geometries. It is also noted that if lumped capacitive coupling is provided by reversed bias varactor-type diodes, the frequency separation between modes can be made electronically tunable through bias-voltage control.

2. DIELECTRIC-SLAB LOADED PARALLEL PLATE WAVE GUIDE

The transverse-electric (TE) modes of a parallel plate region containing a single rectangular dielectric slab of permittivity ε_k and width w as shown in Fig. 3a are well known to have the following non zero field components:

$$H_x = -\frac{\beta}{\omega\mu_o} E_y \tag{1}$$

$$H_z = j\frac{1}{\omega\mu_o}\frac{\partial E_y}{\partial X} \tag{2}$$

where

$$E_y = \begin{cases} E_o \begin{Bmatrix}\cos\\ \sin\end{Bmatrix} kx \quad e^{-j\beta z} & 0 \le x \le w/2 \\ E_o \begin{Bmatrix}\cos\\ \sin\end{Bmatrix} k(x-w/2) \quad e^{-\alpha(x-w/2)} \quad e^{-j\beta z} & w/2 \le x \end{cases} . \tag{3}$$

The even modes have electric fields proportional to cos kx; the odd modes to sin kx.

The eigen-frequencies satisfy

$$\beta^2 + k^2 = \omega^2\varepsilon_k\mu_o \tag{4a}$$

$$\beta^2 - \alpha^2 = \omega^2\varepsilon_\alpha\mu_o \tag{4b}$$

and either

$$\alpha = k \begin{cases} \tan\left(\frac{kw}{2}\right) & \text{even modes} \\ -\cot\left(\frac{kw}{2}\right) & \text{odd modes} \end{cases} \tag{5}$$

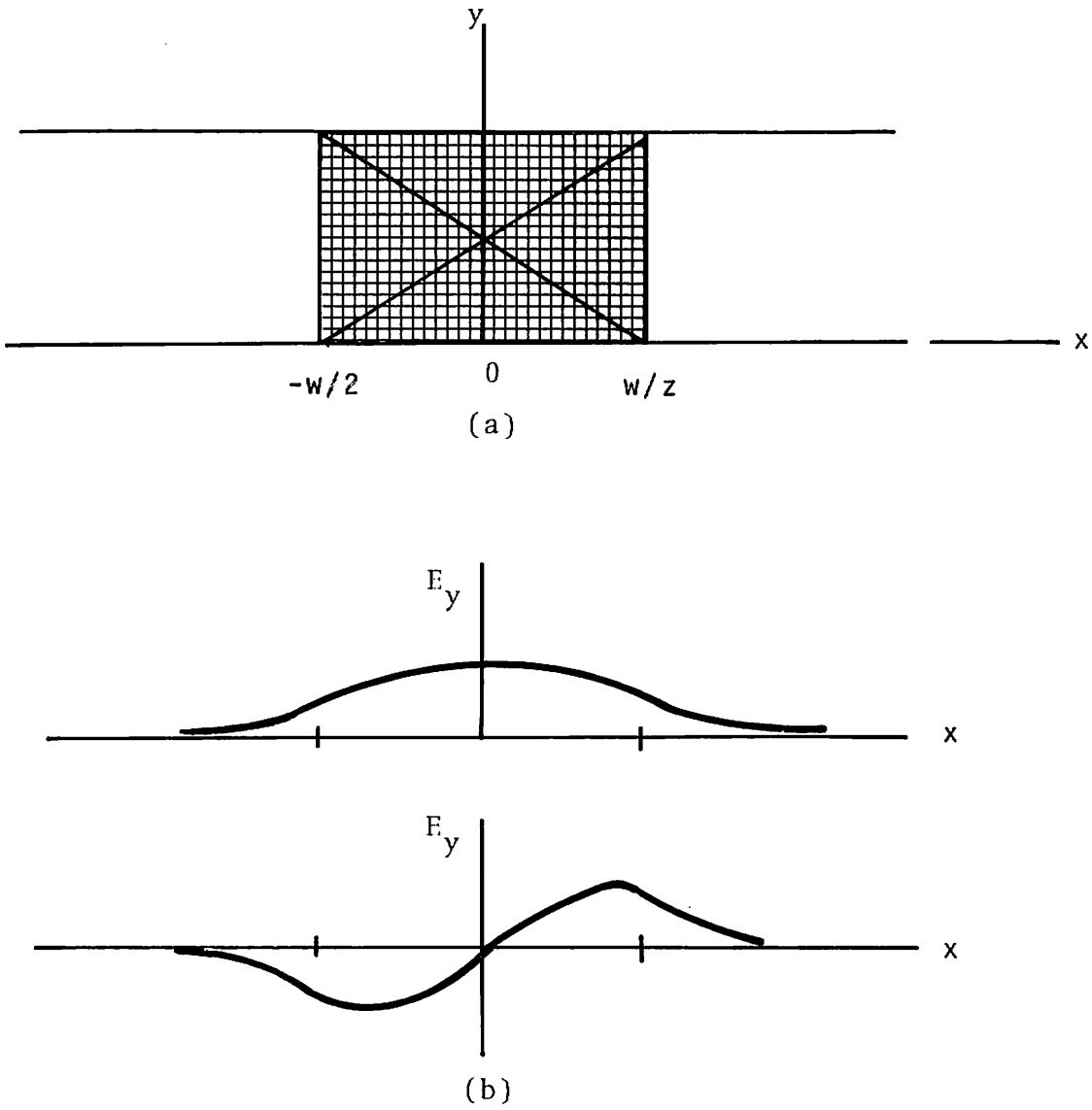

Parallel plates loaded with a dielectric slab are shown in (a) Electric field patterns of the lowest order symmetric and anti-symmetric modes are depicted in (b).

FIGURE 3. PARALLEL PLATES LOADED WITH A DIELECTRIC SLAB

The well known graphical solution is depicted in Fig. 4 and the form of the lowest even and lowest odd modes is sketched in Fig 3b.

As a specific example, assume that

$$\alpha = k = \frac{\pi}{2w} = \frac{2\pi}{\lambda_0}\sqrt{\frac{\varepsilon_k - \varepsilon_\alpha}{\varepsilon_0}} \quad . \tag{6}$$

Because of the exponential decay factor, a second identical dielectric slab placed a distance of several w to the right of the first slab will only weakly disturb the fringing field of the first. It therefore follows that the composite structure has two lowest modes of the same frequency, with energy concentrated either in the left or right slab. Naturally, both slabs may be excited simultaneously and it is then convenient to expand the overall field pattern into even and odd modes of the composite structure; these are shown in Fig. 5a and 5b.

If now the separation between the two slabs is reduced, the fringing fields of the two slabs interact differently according to whether the overall mode is even or odd. This behavior is sketched in Figs. 5c and 5d and causes the frequencies of the two configurations to be split by the interaction. Nevertheless, if, in our example, the separation is reduced no further than w, the exponential decay is still sufficiently great to permit only a weak splitting.

In this manner, one rectangular microstrip patch of length $L = \frac{\pi}{2\beta}$ and overall width 4-5w can support two closely spaced $\lambda/2$ resonances that only weakly fringe at the open edges $|x| = w_t/2$, shown in Fig. 6a,b. Unfortunately, the radiation patterns arising from the open circuit edge (z=0) are not identical for the two modes and, in fact, the odd mode does not even

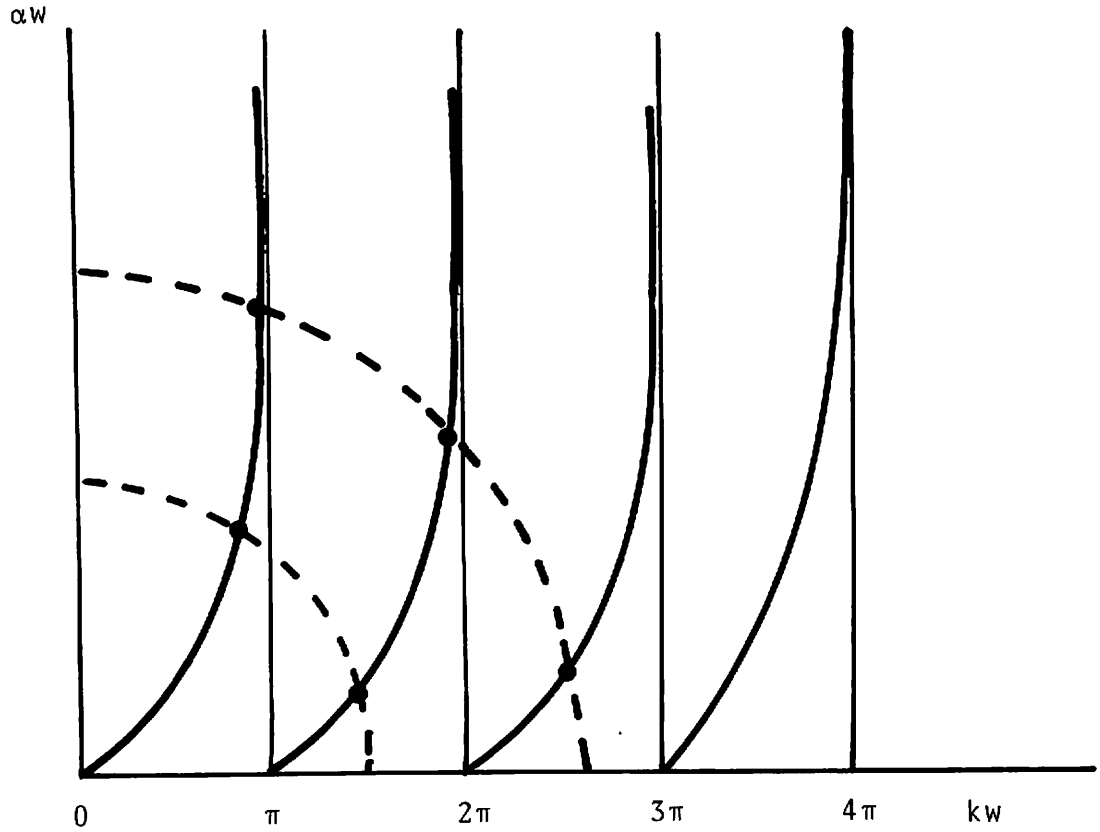

The radii of the dotted circles are proportional to frequency. For the lower of the two frequencies depicted, there are two modes (one symmetric, one antisymmetric). For the higher frequency there are three (two symmetric, one antisymmetric).

FIGURE 4. DIAGRAM USED TO DETERMINE GRAPHICALLY THE MODE VALUES OF α AND k

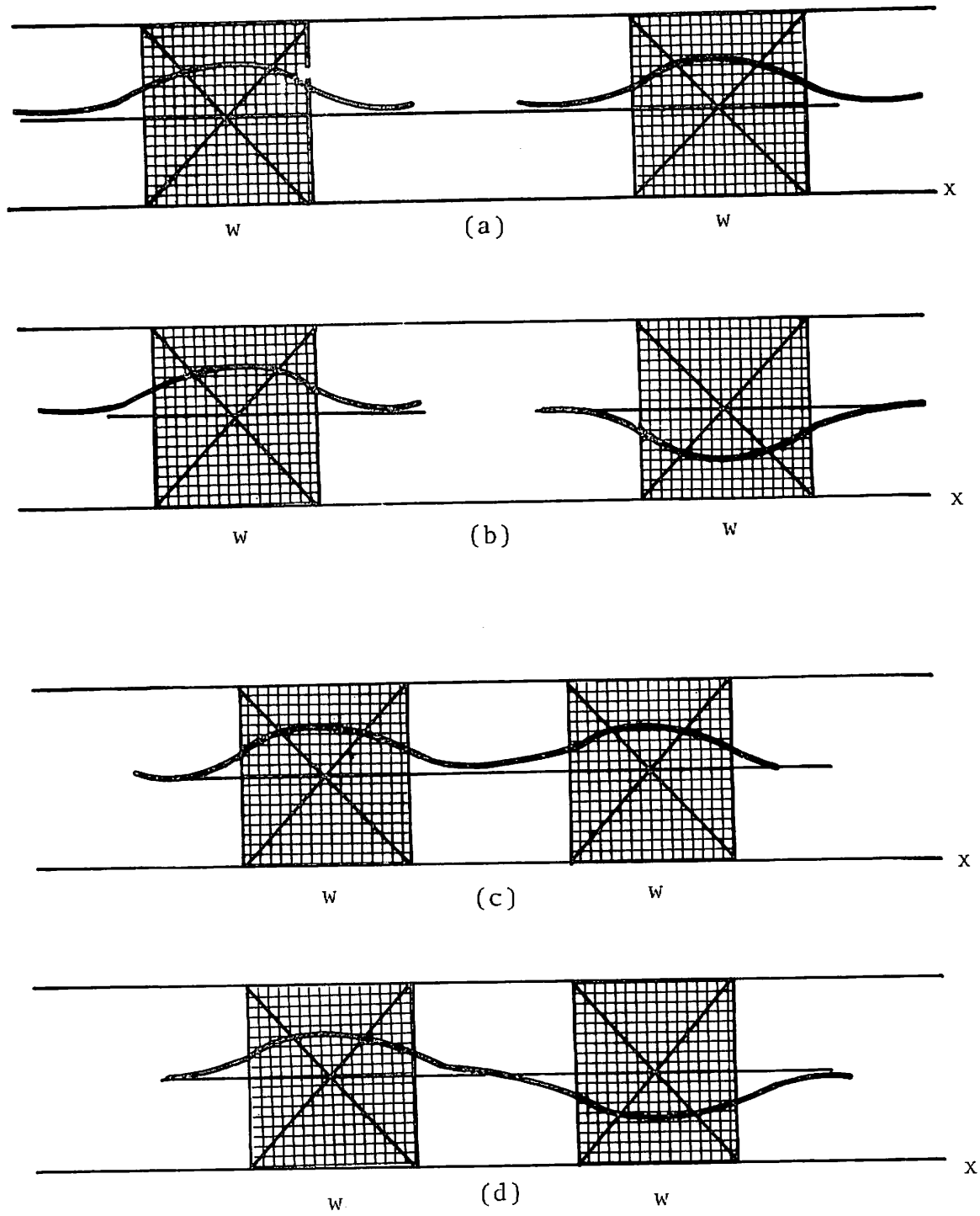

As the slabs are moved together (b) the frequency degeneracy is split by the interaction of the fringing fields.

FIGURE 5. DEGENERATE EVEN AND ODD MODES OF A DOUBLE SLAB LOADED PARALLEL PLATE TRANSMISSION LINE ARE SKETCHED IN (a)

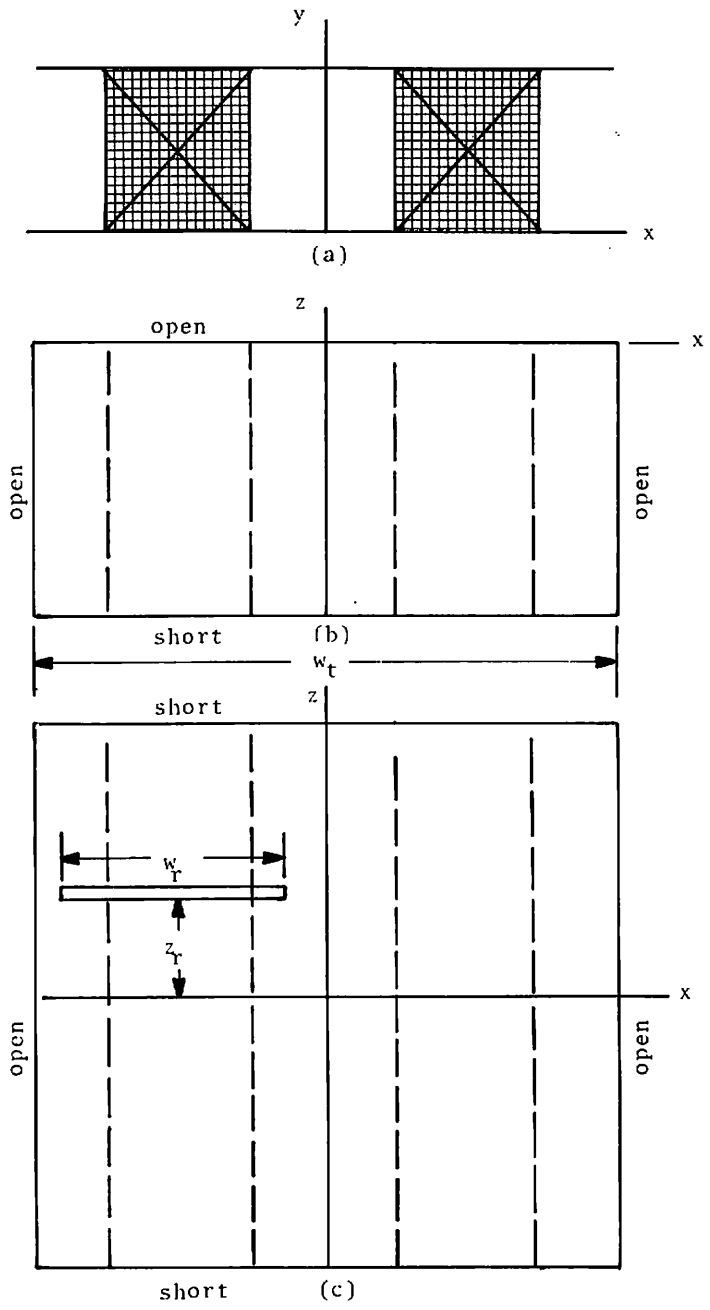

A dual frequency λ/4-resonant microstrip patch element that radiates from the open edge opposite the short circuit is shown in (a) and (b). In (c), to maintain approximately the same radiation pattern for both the even and odd modes, the patch length is doubled and the dual-frequency λ/2 resonant modes both radiate through a slot of length w_r. The power radiated is proportional to the square of the surface current intercepted by the slot.

FIGURE 6. DUAL FREQUENCY MICROSTRIP ELEMENTS EMPLOYING RADIATING SLOTS

radiate in the direction normal to the edge. This condition can be rectified by shorting the edge (after the length has been doubled) and cutting one or more short slots in the top ground plane, as shown in Figure 6.c. The doubling of the length produces $\lambda/2$ rather than $\lambda/4$ resonances; the radiating slot(s) of width $w_r \leq w_t/2$ produce nearly identical patterns and can be designed by standard techniques employed for similar slots used on rectangular wave guide antennas. The radiated power of such a slot is proportional to the square of the total surface current that is interrupted by the slot. As is well known, if the latter is positioned midway between the shorted ends ($z_r = 0$), such current is zero and the slot will not radiate. Note that more than one slot can be employed and the slots may be positioned over either the left or right hand dielectric slab (but not both - unless different radiation patterns are required at the two frequencies).

Finally, more than two closely spaced mode frequencies can be created by employing additional slabs.

2.1 Rectangular Micro-Patch Loaded with Three Dielectric Slabs

When the number of dielectric slabs that are used to load the rectangular microstrip-patch is odd, it is possible to create closely spaced dual resonances with modes that are both spatially even. In such cases, the radiating slots will be located symmetrically which may be desirable in reducing mutual coupling between patches in certain types of arrays.

Although the methods of analysis can be extended to any number of slabs we here restrict ourselves to three symmetrically disposed slabs as shown in Fig. 7., and for simplicity assume that the boundary surfaces at $|x| = w_t/2$

*Fry, D.W., F.K. Goward, Aerials for Centimetre Wave-lengths, Cambridge University Press (1950), p. 110.

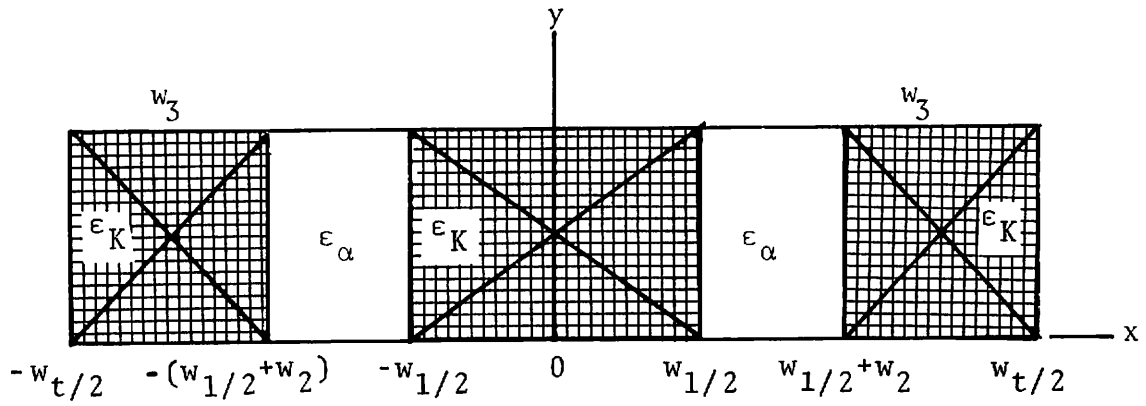

Transverse geometry of the three dielectric-slab configuration analyzed in the text. Multiple slabs permit control of the mode taper.

FIGURE 7. TRANSVERSE GEOMETRY OF THE THREE DIELECTRIC-SLAB CONFIGURATION

are perfect open circuits electromagnetically.

Straightforward application of equations similar to Eqs. (1) - (3) in each of the five regions (except that both $e^{\pm\alpha x}$ terms are required in the two ε_α regions) gives an electric field E_y that has a pattern for even modes that is proportional to $f(x) = f(-x)$ given by

$$f(x) = \begin{cases} \cos k_x & 0 \le x \le w_{1/2} \\ A(e^{-\alpha x} + \Gamma e^{\alpha x}) & w_{1/2} \le x < w_{1/2} + w_2 \\ B \cos k(\frac{w_t}{2} - x) & \frac{w_1}{2} + w_2 \le x \le \frac{w_1}{2} + w_2 + w_3 = w_t/2 \end{cases} \tag{7}$$

where

$$A = \frac{1}{2} e^{\frac{\alpha w_1}{2}} \cos \frac{k w_1}{2} \left(1 + \frac{k}{\alpha} \tan \frac{w_1}{2}\right) \tag{8}$$

$$B = \frac{1}{2} \frac{\cos\left(\frac{k w_1}{2}\right)}{\cos k w_3} \left[\left(1 + \frac{k}{\alpha} \tan \frac{w_1}{2}\right) e^{-\alpha w_2} + \left(1 - \frac{k}{\alpha} \tan \frac{k w_1}{2}\right) e^{\alpha w_2}\right] \tag{9}$$

$$\Gamma = e^{-\alpha w_1} \frac{1 - \frac{k}{\alpha} \tan \frac{k w_1}{2}}{1 + \frac{k}{\alpha} \tan \frac{k w_1}{2}} \tag{10}$$

$$\alpha^2 + k^2 = \Delta\varepsilon' \left(\frac{2\pi}{\lambda_o}\right)^2 ; \quad \Delta\varepsilon' = \varepsilon_k' - \varepsilon' > 0 \tag{11}$$

$$\beta = \sqrt{\varepsilon_k' k_o^2 - k^2} \tag{12}$$

The values of α and k must also satisfy the following transcendental relationship

$$\frac{\alpha}{k}\,\frac{\frac{\alpha}{k}\tanh\,\alpha w_2 - \tan kw_3}{\tanh\,\alpha w_2 \tan kw_3 - \frac{\alpha}{k}} + \begin{cases} \tan\frac{kw_1}{2} \\ -\cot\frac{kw_1}{2} \end{cases} = 0 \qquad \begin{matrix} \text{even modes} \\ \\ \text{odd modes} \end{matrix} \qquad (13)$$

2.2 RADIATION PATTERNS FROM EVEN MODES

The radiation pattern associated with the even mode distribution $f(x) = f(-x)$ follows from

$$P(\theta) = 2\cos\theta \int_0^{w_{t/2}} f(x)\cos(k_o x \sin\Phi)\,dx \qquad (14)$$

where $k_o = 2\pi/\lambda_o$ and λ_o is the free space wavelength.

The result of the integration is

$$P(\theta) = \left\{k_o B[\cos(k\ell_3)(f_3 - f_2) - \sin(k\ell_3)(g_3 - g_2)] + f_1 - \frac{2Ak_o}{\alpha^2 + k_o^2\sin^2\theta}(h_1 - h_2)\right\}\cos\theta \qquad (15)$$

with

$$f_i = \frac{\sin[(k_o\sin\theta + k)w_i]}{k_o\sin\theta + k} + \frac{\sin[(k_o\sin\theta - k)w_i]}{k_o\sin\theta - k} \qquad (16)$$

$$g_i = \frac{\cos[(k_o\sin\theta + k)w_i}{k_o\sin\theta + k} - \frac{\cos[(k_o\sin\theta - k)w_i}{k_o\sin\theta - k} \qquad (17)$$

and

$$h_i = (\Gamma e^{\alpha w_i} - e^{-\alpha w_i})\,\alpha\cos(w_i k_o\sin\theta) + (\Gamma e^{\alpha w_i} + e^{-\alpha w_i})\,k_o\sin\theta\sin(w_i k_o\sin\theta)\,. \qquad (18)$$

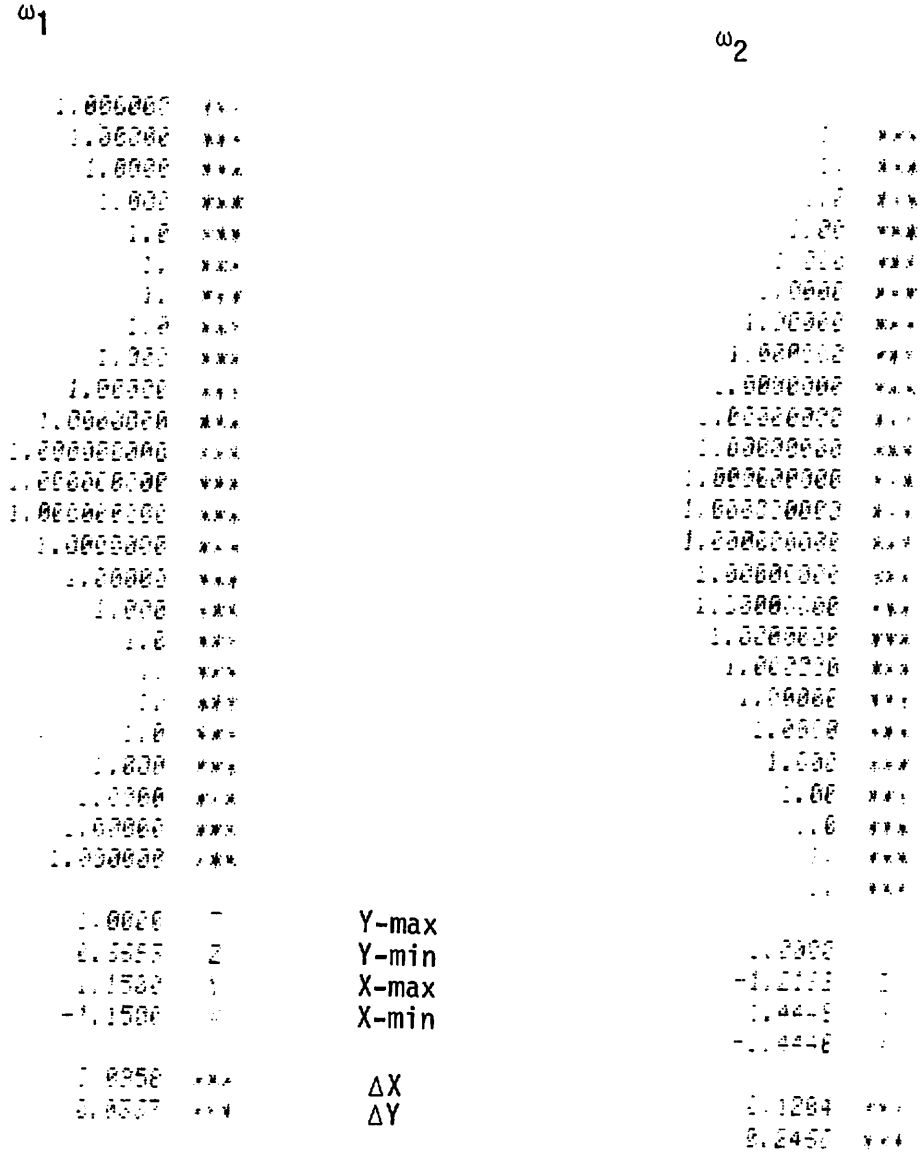

Computer graphs of the mode amplitude for the dual resonances used as an example of the three slab configuration. The frequency separation is 25 percent.

FIGURE 8. MODE AMPLITUDES FOR DUAL RESONANCES IN THE THREE SLAB STRUCTURE

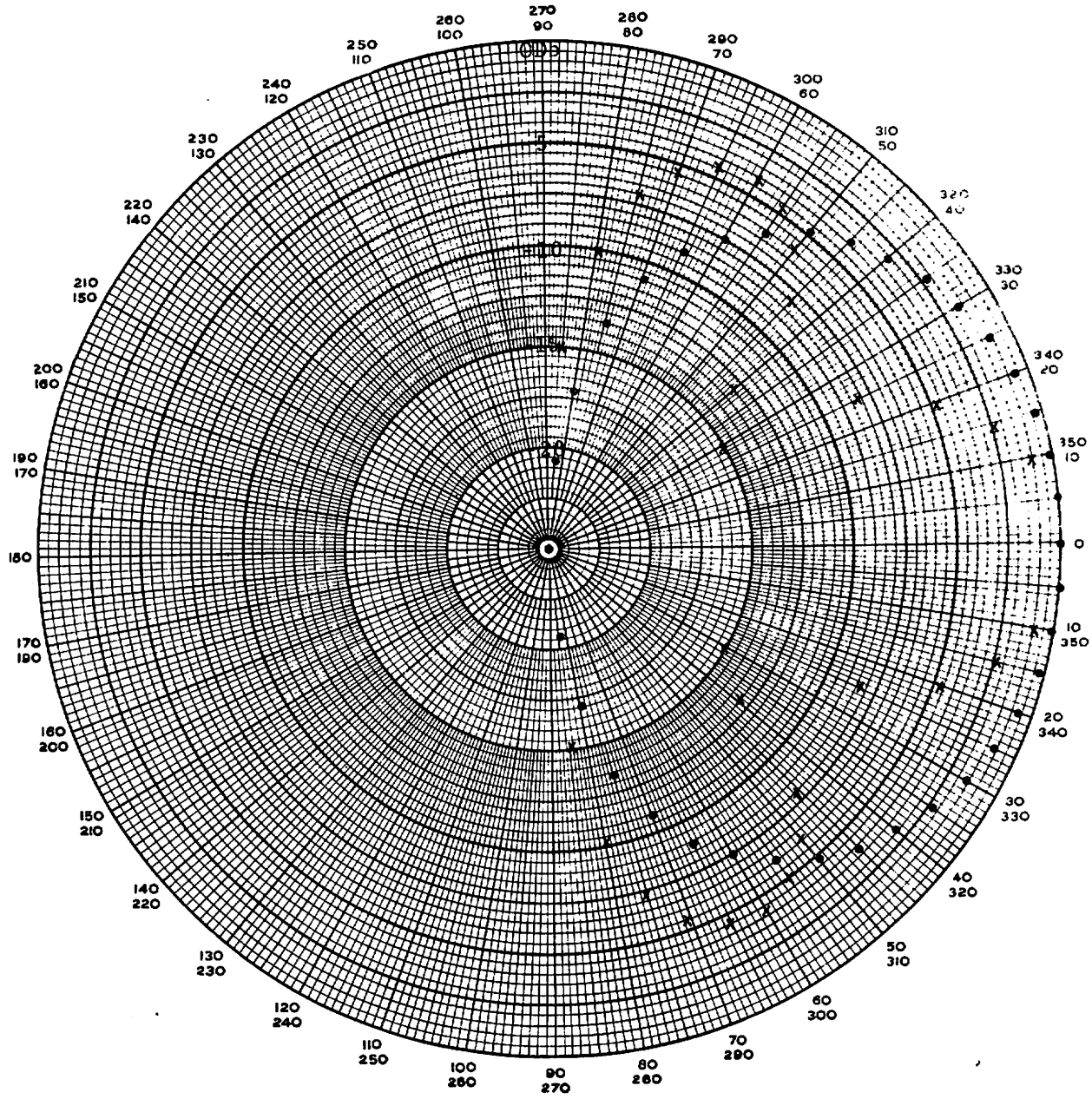

Polar radiation diagram for the modes of Fig. 8 when $w_r = w_t$. The differences can largely be eliminated by reducing w_r.

FIGURE 9. POLAR RADIATION DIAGRAM (1)

Example

For purposes of illustration, consider a three slab design with the following parameters:

$$\varepsilon_k' = 10$$
$$\varepsilon_\alpha' = 1.5$$
$$w_t/L = 3.81$$
$$w_1:w_2:w_3 = 7:5:3 \quad .$$

The dual resonance mode parameters are found to be:

Lower frequency	Higher frequency
$k/k_{01} = 1.795$	$k/k_{02} = 2.389$
$\alpha/k_{01} = 2.298$	$\alpha/k_{02} = 1.671$
$\beta/k_{01} = 2.604$	$\beta/k_{02} = 2.889$

where $k_{02}/k_{01} = \omega_2/\omega_1 = 1.26$.

The mode distributions f(x) are plotted in Fig. 8 and the corresponding radiation patterns, plotted in Fig. 9 for $w_r = w_t$.

Notice that, although both mode distributions are even functions, the radiation patterns for the two modes are significantly different. This can be corrected by simply reducing the radiating aperture w_r to the central one-half or one-third of w_t. The associated broadening of the main peak is beneficial for many applications.

Although the fabrication of microstrip patches loaded with multiple dielectric slabs poses practical problems of fabrication, special requirements which are met by designs employing such techniques may warrant their consideration. However, the next case considered is of considerable practical

importance and involves no fabrication difficulties beyond those encountered in conventional microstrip elements.

2.3 SINGLE DIELECTRIC MICRO-PATCH

The previous analysis can be employed for a single slab by setting $w_3 = 0$, and when the micropatch is completely filled, $w_2 = 0$.

In this case,

$$k_1^2 + \beta_1^2 = \omega_1^2 \mu_o \varepsilon_k \tag{19a}$$

$$k_2^2 + \beta_2^2 = \omega_2^2 \mu_o \varepsilon_k \quad . \tag{19b}$$

The lowest order modes require $k_1 = 0$, $k_2 = \pi/w_t$ and $\beta_1 = \beta_2 = \pi/L$.

Hence,

$$L = \frac{\lambda_{01}}{2\sqrt{\varepsilon_k'}} \tag{20a}$$

where

$$\lambda_{01} = \lambda_0 \text{ for } w_1$$

$$w_t = L / \sqrt{\left(\frac{\omega_2}{\omega_1}\right) - 1} \quad . \tag{20b}$$

Provided the required frequency separation $(\omega_2 - \omega_1)$ is not too small, practical configurations are available. As an example, consider a design requirement of $\frac{\omega_2}{\omega_1} = 1.1$, $\varepsilon_k' = 9$. In this case, $L = \lambda_{01}/6$, and the total area of the patch is

$$w_t L = .06\, \lambda_{01}^2$$

which is slightly less than would be required for a $\lambda_{01}/4$ square patch if $\epsilon_k' = 1$.

The radiation pattern follows from

$$P(\theta) \sim \int f(x)\, e^{j(k_o \sin\theta X)}\, dx$$

where for ω_1, $f(x) = 1$ (even mode)

and; for ω_2, $f(x) = \sin \frac{\pi x}{w_t}$ (odd mode).

That is to say, the excitation is constant for the even mode and sinusoidal for the odd mode.

When normalized to the value at $\theta = 0$, $\rho(\theta)$ is given by

$$\text{(odd mode)} \qquad p^2(\theta) = \left(\frac{\cos\theta}{2\,\frac{\sin k w_r}{k w_r}}\right)^2 \left\{ \left(\frac{\sin[(k_o \sin\theta + k)\,\frac{w_r}{2}]}{[(k_o \sin\theta + k)\,\frac{w_r}{2}]} \right)^2 + \left(\frac{\sin[(k_o \sin\theta - k)\,\frac{w_r}{2}]}{[(k_o \sin\theta - k)\,\frac{w_r}{2}]} \right)^2 + 2\cos(k w_r)\, \frac{\sin[(k_o \sin\theta + k)\frac{w_r}{2}]\, \sin[(k_o \sin\theta - k)\frac{w_r}{2}]}{[(k_o \sin\theta + k)\frac{w_r}{2}]\, [(k_o \sin\theta - k)\frac{w_r}{2}]} \right\}$$

$$\text{(even mode)} \qquad p^2(\theta) = \cos\theta\, \frac{\sin(k_o \sin\theta\ w_r)}{k_o \sin\theta\ w_r/2} \qquad (21)$$

For the example chosen, the patterns are plotted for both $k_1 = 0$ and $k_2 = \pi/w_t$ in Fig. 10 when $w_r = w_t$ and in Fig. 11 when w_r corresponds to the left (or right) one-half of w_t. The element geometry is that of Fig. 6c except that only a uniform dielectric is used as in conventional microstrip.

The importance of this result should be noted here. Using a single layer microstrip structure with commonly used fabrication techniques, including plated-through holes, the preceding analysis shows that by adjusting patch and slot parameters it is possible to produce nearly identical radiation patterns at two frequencies separated by at least 5-10 percent.

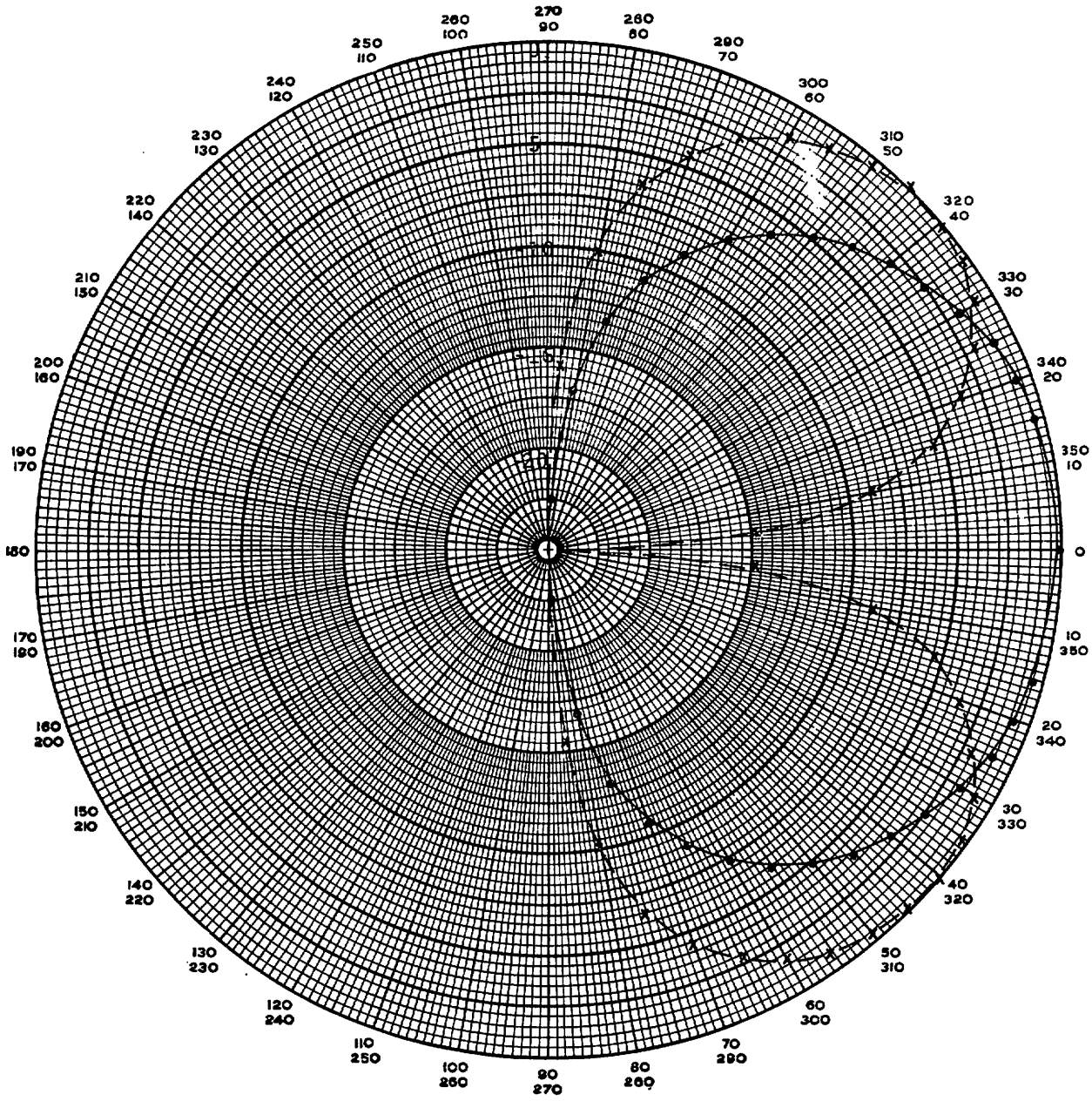

Polar radiation diagram for a single microstrip patch dielectric-filled microstrip patch designed with dual resonances separated by 10 percent when $w_r = w_t$. Differences between the patterns for the two modes are appreciable.

FIGURE 10. POLAR RADIATION DIAGRAM (2)

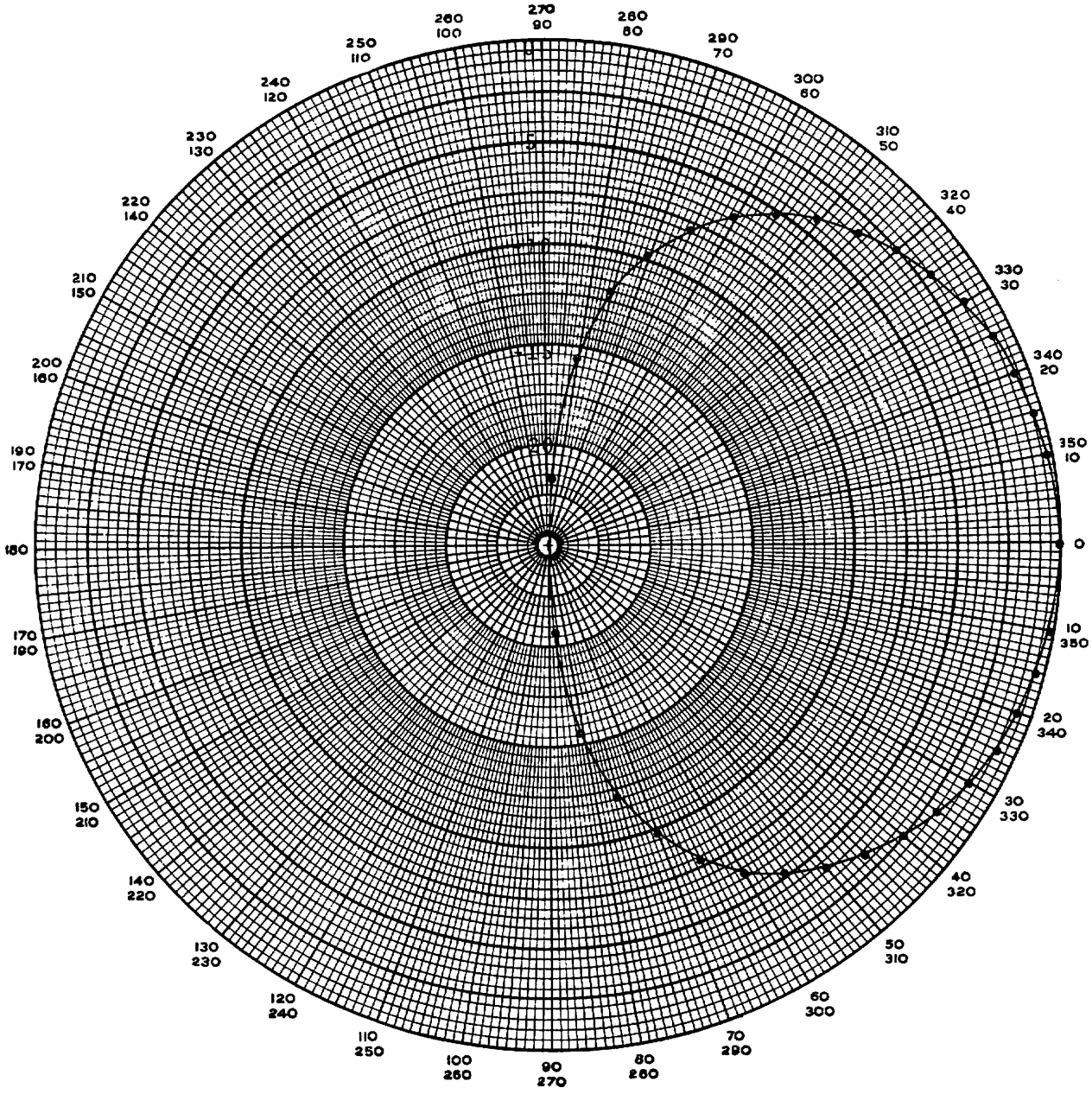

Polar radiation diagram for a single microstrip patch dielectric-filled microstrip patch designed with dual resonances separated by 10 percent when $w_r = w_{t/2}$. Differences between the patterns for the two modes are negligible.

FIGURE 11. POLAR RADIATION DIAGRAM (3)

Radiation efficiency of the two modes (frequencies) should be comparable since the currents intercepted by the slot are comparable at the two frequencies. Achieving this inherent efficiency depends on the efficiency with which the element feed couples to the two modes inside the element. Although an analysis of the feed has not been carried out in detail, inspection of the mode structure shows that a feed point should be available which is a good compromise for the two modes, and which will allow the element to be matched using standard techniques.

3. DUAL-FREQUENCY MODES OF COUPLED RESONATORS

In this section, a synthesis approach based upon coupled resonator theory is developed and applied to purely distributed circuits and also to hybrid circuits employing supplementary lumped elements.

3.1 LUMPED-CIRCUIT MODEL

A lumped circuit model that is very useful for understanding coupled resonances is given in Fig.12a.

If $L_1C_1 \neq L_2C_2$ and the coupling capacitor C_o is small, the two resonance frequencies are well separated and, at each, only one of the tank circuits will be excited to any appreciable extent. If these resonators represent radiating microstrip patches, their design can be carried out independently.

When the frequencies are desired to be closely spaced with the coupling element of a weak or moderate strength, it is necessary that the uncoupled resonances ($C_o = 0$) be nearly equal.

For simplicity, we set

$$L_1C_1 = L_2C_2 = 1/\omega_a^2 \tag{22}$$

and immediately resolve the circuit excitations into modes in which the voltages v_1 and v_2 are either in phase or out of phase.

The in-phase mode has $v_1 = v_2$; since no current or voltage appears across C_o it may be removed as shown in Fig. 12b. Evidently, the frequency is given by $\omega = \omega_a$.

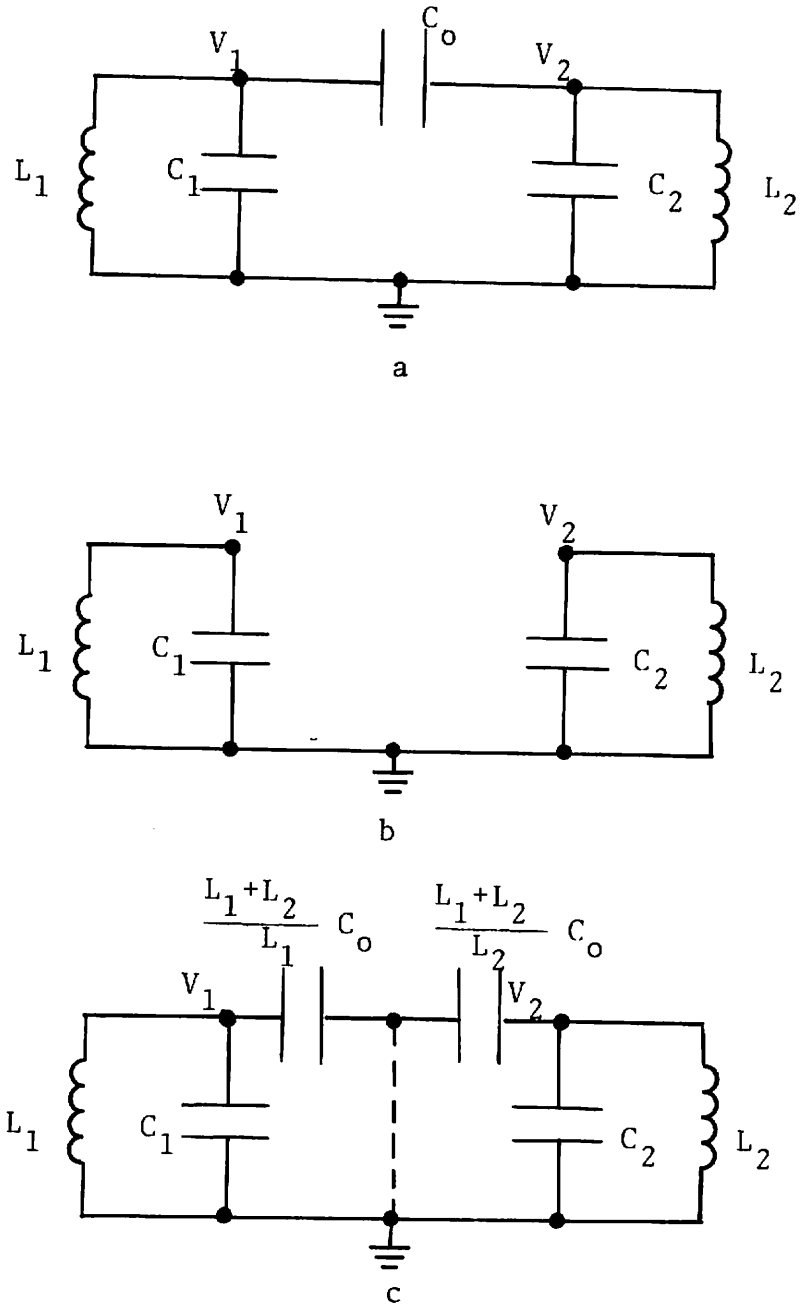

The coupled-lumped circuit model used to analyze dual resonances is shown in (a). The circuit applicable to the "in-phase" mode is given in (b); that to the "out-of-phase" mode in (c).

FIGURE 12. THE COUPLED-LUMPED CIRCUIT MODEL USED TO ANALYZE DUAL RESONANCES

The out-of-phase mode is most easily analyzed from the circuit of Fig. 12c in which C_o has been replaced by two series connected capacitors chosen so that their common connection is at ground potential. Hence,

$$L_1[C_1 + (1+\frac{L_2}{L_1})C_o] = L_2[C_2 + (1 + \frac{L_1}{L_2})C_o] = \frac{1}{\omega_b^2} \tag{23}$$

and because the current through each must be identical, it follows that $C_1 v_1 = -C_2 v_2$.

The frequency of this mode is $\omega = \omega_b < \omega_a$.

The value of C_o necessary to provide the appropriate frequency splitting is found from

$$(L_1 + L_2)C_o = \frac{1}{\omega_b^2} - \frac{1}{\omega_a^2} \quad . \tag{24}$$

Notice that the impedance levels $\sqrt{\frac{L_1}{C_1}}$ and $\sqrt{\frac{L_2}{C_2}}$ can be set independently even though $\sqrt{L_1C_1} = \sqrt{L_2C_2}$. When the impedances are very dissimilar, the stored energy associated with each mode will principally reside in <u>one</u> of the two tank circuits; when identical, the energy will be equally divided. This consideration is a very important factor in the design of efficient dual-frequency microstrip radiators.

It is helpful at this point to define two classes of capacitively-coupled circuits. In the first type, one of the tank circuits is provided by a resonant microstrip patch; in the other a non-radiating matching circuit is made from lumped elements.

In the second type, both tank circuits are resonant microstrip patches.

3.2 DISTRIBUTED-LUMPED MODEL

In this type, the radiating element comprises an edge or slot(s) of the micro-patch. Because the patch must be strongly excited for the modes of both frequencies, it is necessary that the impedance levels of the two tank circuits be approximately equal.

If the length ℓ of the patch is $\lambda/4$ within the dielectric substrate at the frequency ω_a it follows from the circuit of Fig. 13 that

$$\omega_a = \pi/2 \Big/ \sqrt{L'C'}\,\ell = 1/\sqrt{L_2C_2} \tag{25}$$

for the "in-phase" resonance, and an "out-of-phase" resonance at ω_b controlled by C_o according to

$$\frac{C_o}{C_2} = \frac{1 - (\omega_b/\omega_a)^2}{(\omega_b/\omega_a)^2 + Z_o\,\omega_b C_2 (1 - \omega_b^2/\omega_a^2)\tan\left(\frac{\pi}{2}\,\frac{\omega_b}{\omega_a}\right)} \tag{26}$$

In the vicinity of ω_a, the lumped equivalent circuit of the transmission line is a parallel L-C circuit with elements identical to the lumped circuit on the right hand side provided that

$$C_1 = \frac{1}{2}\,C'\ell = C_2$$

and

$$L_1 = \frac{8}{\pi^2}\,L'\ell = L_2 \quad .$$

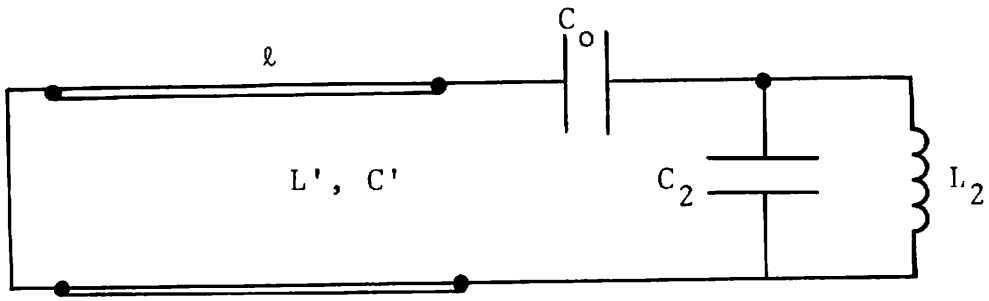

The distributed-lumped resonance circuit model replaces L_1, C_1 with a short-circuited transmission line.

FIGURE 13. THE DISTRIBUTED-LUMPED RESONANCE CIRCUIT MODEL

Here C' and L' are respectively the per unit length values of the microstrip capacitance and inductance. When h/w <<1, they are approximately given by

$$C' \simeq \frac{\varepsilon w}{h} \tag{27a}$$

and

$$L' = \mu_o \frac{h}{w} \quad . \tag{27b}$$

More accurate formulas are available in Appendix A of Volume I of this report.

3.3 DISTRIBUTED-DISTRIBUTED MODEL

In this type, the radiating elements can be located on only one of the patches or on both patches. In the former case, the radiation patterns can be made essentially identical if the aperture distributions of the radiating elements are nearly alike at both frequencies. Obviously, for good efficiency, the radiating patch must be highly excited at both frequencies and this implies that the impedance levels of the two patches must be nearly the same.

In the latter case, because of the phase difference between the ω_a and ω_b modes, it is essential that only a single patch radiate at either frequency.

This can be accomplished by intentionally mismatching the characteristic impedances of the two patches, so as to greatly reduce energy density and the radiation of one of the patches.

The resonance frequencies of the circuit shown in Fig. 14 satisfy

$$Y_{01}\cot\beta_1\ell_1 = \frac{\omega C_o}{1 - \omega C_o Z_{02} \tan\beta_2\ell_2} \tag{28}$$

where $\beta_i = \omega\sqrt{L_i'C_i'}$ and $Z_{oi} = 1/Y_{oi} = \sqrt{L_i'/C_i'}$.

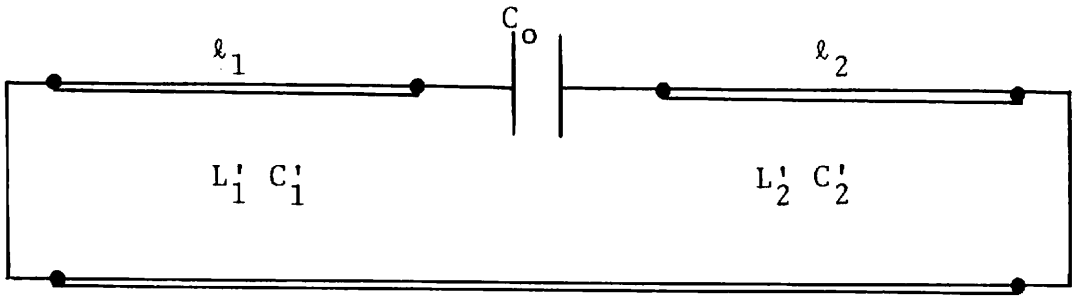

The distributed-distributed circuit model replaces both L_1,C_1 and L_2,C_2 with short-circuited transmission lines.

FIGURE 14. THE DISTRIBUTED-DISTRIBUTED RESONANCE CIRCUIT MODEL

If $\beta_1 = \beta_2 = \beta$ and $Y_{01} = Y_{02} = Y_0$

$$Y_0 \cot\beta\ell = \frac{\omega C_o}{1 - \omega C_o Z_o \tan\beta\ell} \quad . \tag{29}$$

In this case, $\omega_a \sqrt{L'C'}\,\ell$ and $\omega_b < \omega_a$ is controlled by

$$C_o = \frac{1}{2} Y_o \frac{1}{\omega_b} \cot\left(\frac{\omega_b}{\omega_a}\frac{\pi}{2}\right) \quad . \tag{30}$$

3.4 COMPOSITE TRANSMISSION LINE SECTIONS

Additional flexibility is gained by dividing any transmission line of the above-mentioned circuits into two or more sections. As an illustration, consider the composite line of Fig. 15 made up of two sections having, in general, different characteristic impedances and propagation constants.

The input impedance of the composite is

$$Z_{in} = j \frac{Z_{01}\tan\beta_1\ell_1 + Z_{02}\tan\beta_2\ell_2}{1 - \frac{Z_{01}}{Z_{02}} \tan\beta_1\ell_1 \tan\beta_2\ell_2} \quad . \tag{31}$$

For "in-phase" modes where $\omega = \omega_a$, Z_{in} is an open-circuit and

$$\tan\beta_1\ell_1 \tan\beta_2\ell_2 = \frac{Z_{02}}{Z_{01}} \tag{32}$$

The minimum physical length $\ell_t = \ell_1 + \ell_2 \leq \pi/2\beta_{max}$ is found from

$$\beta_1 \sin(2\beta_2\ell_2) = \beta_2 \sin(2\beta_1\ell_1) \tag{33}$$

provided this constraint is compatible with Eq. (32). If no such solution exists, the minimum length occurs when the line consists of a single section having the maximum value of β.

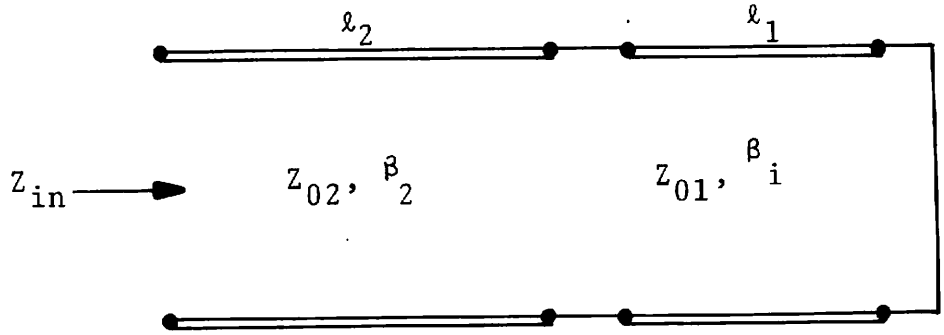

FIGURE 15. A COMPOSITE VERSION OF THE SHORT-CIRCUITED TRANSMISSION LINE

If $\beta_1 = \beta_2 = 2\pi/\lambda$, Eq. (33) implies $\ell_1 = \ell_2$ and

$$\ell_t = \frac{\lambda}{\pi} \tan^{-1} \sqrt{\frac{Z_{02}}{Z_{01}}} \quad .$$

When $Z_{02} < Z_{01}$, it is seen that $\ell_t < \lambda/4$. For example, if $Z_{01} = 2Z_{02}$, $\ell_t = .196\lambda$; for $Z_{01} = 3Z_{02}$, $\ell_t = .167\lambda$.

If the dielectric constant of both lines is the same, changes in Z_o require a change in the h/W ratio; the resultant discontinuity also places a shunt reactance across the junction between sections which we have neglected for the sake of simplicity.

For microstrip lines deposited upon uniform dielectric substrates of constant thickness, h, the control of Z_o is through the strip width W. As long as $h/w \ll 1$, the values of β are essentially independent of Z_o.

Because, for length reduction, we wish $w_2 > w_1$, the reduced width line can be folded to occupy still less area. This process is shown in Fig. 16a,b where the heavy solid line represents the short circuit termination to the bottom ground plane. Naturally, the patch can be subdivided into strips, each similarly treated as sketched in Fig. 16c. Notice that the conductor along the line shown dotted may be kept either solid or slotted.

Alternatively, the slots may be cut at an angle as shown in Fig. 16d. Such geometries provide tapered values of Z_o that reduce shunt junction reactances and also allow the short-circuit termination to be kept along an outside edge.

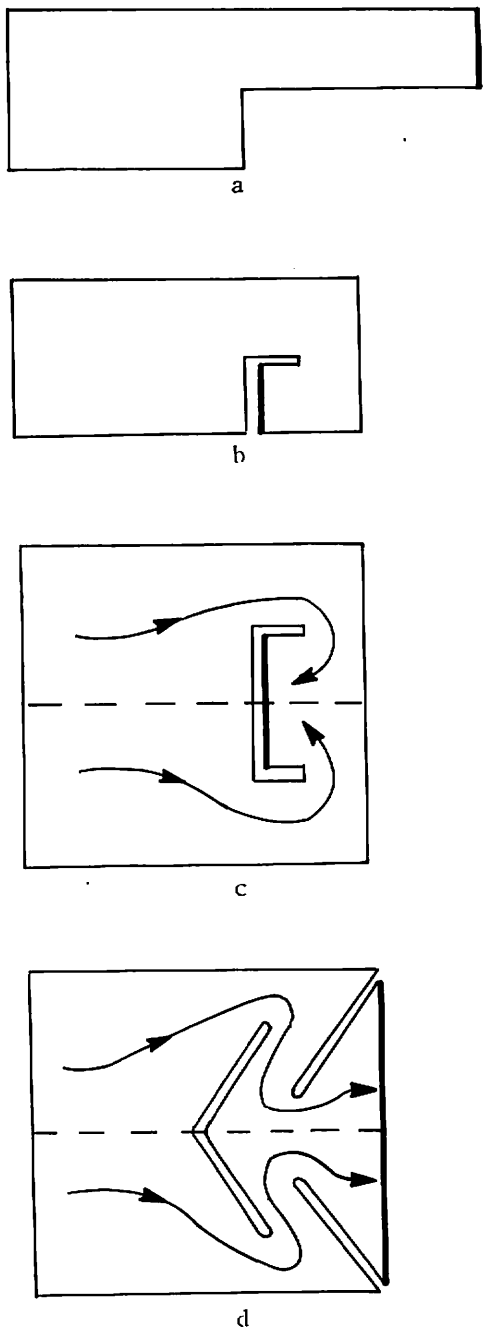

The upper conductor is pictured in each case with the terminating short-circuits indicated by bold solid lines. The two-section line of Fig. 15 is realized in normal (a) and folded (b) configurations. A rectangular patch is subdivided in (c) and (d) with the arrows schematically indicating the direction of current flow. The dotted lines indicate the positions of optional slots.

FIGURE 16. MICROSTRIP VERSIONS OF THE COMPOSITE TRANSMISSION LINE

4. DUAL-RESONANCE MICROSTRIP ANTENNA CONFIGURATIONS

The principles described above can be utilized to create a variety of novel radiating elements.

Several distributed versions are depicted in sectional views in Figs. 17 to 19. The first two of these are in-line distributed-distributed circuits in which the radiation is produced from one or more slots in one of the patches. Notice that there will be relatively little radiation from the gaps between the patches because the voltage differences are small for the "in-phase" mode, and large, but of opposite polarity for the "out-of-phase" mode. If it is necessary to suppress these small components, the configuration of Fig. 19 can be used which is essentially a stacked-array completely shielded along the top except at the desired radiating slots.

The middle ground planes in the Fig. 19 structure can be identical to, or a variant of Fig. 16. By enclosing such slotted plates between ground planes, radiation from the slots is greatly suppressed. Alternatively, such a plate could be made the top patch of one side of the structure provided the slots were designed so as to also provide the appropriate radiation characteristics.

Lumped capacitors can be shunted across the coupling elements that couple the two sides of any of these dual-frequency antennas so as to affect the value of C_o. If such capacitors are reverse-biased diodes of the varactor type, the frequency separation between the dual resonances can be electronically-controlled.

Finally, we note that there is a unity between the approaches given in Sections 2 and 3 in that the dielectric slab loading produces coupled resonances in which even and odd transverse field distributions play the role of separate distributed transmission lines. In effect, the distributed transmission lines of Fig. 14 are placed side-by-side, rather than in the stacked

The electric field patterns of the "in-phase" and "out-of-phase" modes are shown in (a) and (b) respectively. The left-most slot in the top patch controls the radiation.

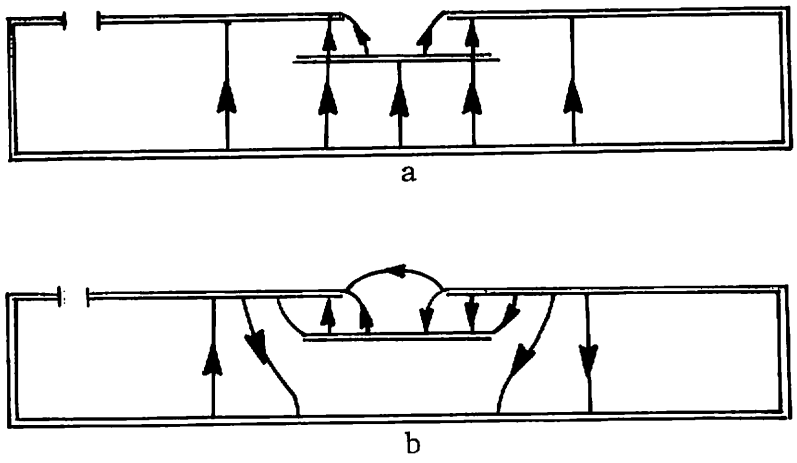

FIGURE 17. SIDE VIEW OF DUAL-FREQUENCY MICROSTRIP PATCH ANTENNA DESIGNED FROM COUPLED RESONATOR THEORY (1)

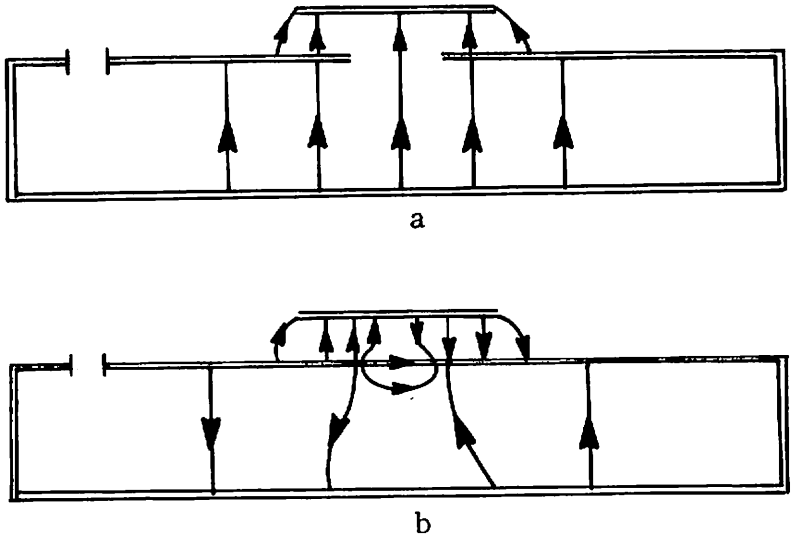

FIGURE 18. SIDE VIEW OF DUAL-FREQUENCY MICROSTRIP PATCH ANTENNA DESIGNED FROM COUPLED RESONATOR THEORY (2)

Because several new design concepts have been proposed, it is important to test them experimentally and compare the results against the theoretical expectations.

We especially recommend that the theoretical analysis and synthesis of appropriate feed networks be carried out for the new antenna designs and that the most promising of these be built, measured and compared to designs currently available in the literature.

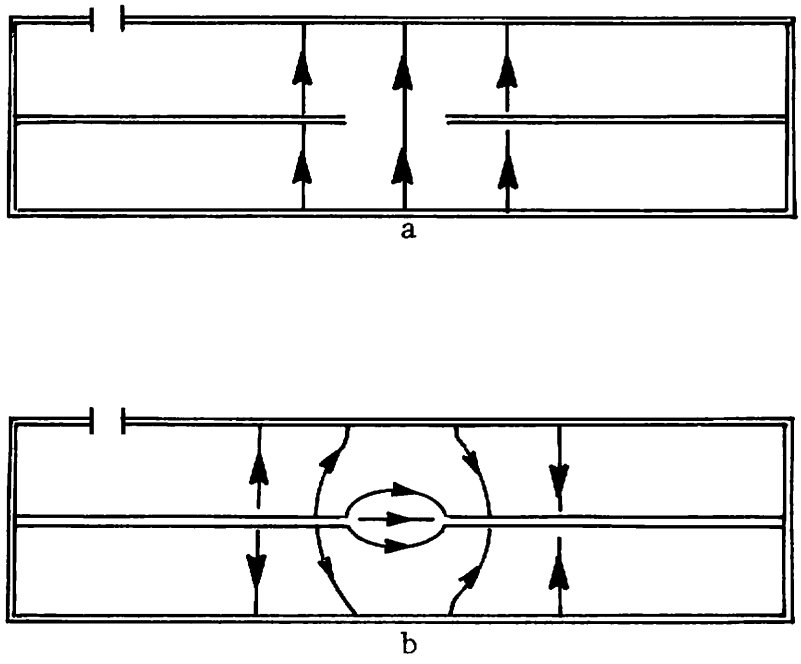

The electric field patterns of the "in-phase" and out-of-phase" modes are shown in (a) and (b) respectively. The left-most slot in the top patch controls the radiation.

FIGURE 19. SIDE VIEW OF A DUAL-FREQUENCY MICROSTRIP PATCH ANTENNA WITH THE MODE COUPLING SLOTS SHIELDED

arrangement of Fig. 19. It is possible to envisage applications in which both techniques are used simultaneously, for example when more than two resonant frequencies are desired.

5. CONCLUSIONS AND RECOMMENDATIONS

In this second volume of the final report, we have discussed and analyzed several approaches aimed at developing rational designs for dual-frequency resonant microstrip patch antennas.

Rather than design the dual-resonating elements and matching networks separately in the hope of achieving efficient radiation and proper patterns at both frequencies, we favor and have here advocated an integrated approach in which both design goals are achieved simultaneously.

In particular, we developed a theoretical model to describe the approximate electromagnetic mode structure of a rectangular patch loaded symmetrically with up to three dielectric slabs that serve to concentrate the rf energy.

Both even and odd modes were considered and the modal field distributions used to derive the radiation pattern produced by a radiating edge or a slot in the top plate of a multi-resonant rectangular patch.

Dual resonances in rectangular microstrip patch filled with homogeneous dielectric appear to be practical when the desired separation between frequencies is at least 5 - 10 percent.

A synthesis approach, based upon coupled resonator theory, was also developed and applied to situations in which one resonant element is a rectangular microstrip patch and the second element either a second patch or else a lumped or distributed matching network. Based upon these considerations, several new antenna configurations were proposed that utilize either in line or stacked element geometries. It was noted that if lumped-capacitive coupling is provided by reversed-bias varactor-type diodes, the frequency separation between modes can be made electronically tunable through bias-voltage control.

APPENDIX - REPORT OF NEW TECHNOLOGY

Several novel configurations of microstrip antennas consisting of one or more slot loaded rectangular patches coupled to either lumped or distributed matching networks are proposed in Vol. II of this report and they should be reviewed by the DOT with respect to patentability.

In addition, certain advances in the theory of multi-frequency microstrip antennas are reported here.

Rather than separately design the dual-resonating elements and matching networks and hope for efficient radiation and proper patterns at both frequencies, we favor and herein pursue an integrated synthesis which demands simultaneous fulfillment of the design goals.

220 copies